

Chapter 28

Pre-Main-Sequence Contraction

In the last section we left the newly born star while it was still contracting in hydrostatic, but not yet thermal, equilibrium. Essential features of this contraction can already be understood by assuming simple homologous changes. It will turn out that the fate of such a sphere is mainly determined by the equation of state.

28.1 Homologous Contraction of a Gaseous Sphere

A star which has not yet reached the temperature for nuclear burning has to supply its energy loss by contraction. This is a consequence of the virial theorem and of energy conservation as discussed in Sect. 3.1. We have seen, in particular, that part of the released gravitational energy goes into internal energy, while the rest supplies the luminosity [see (3.12)]. The characteristic timescale is τ_{KH} , as shown in Sect. 3.3.

In the following we will be concerned with the centre of the star. For this we can use the relations of Sect. 20.3, which hold for any mass shell of a homologously contracting star. The equation of state (for fixed chemical composition) was written there as $d\varrho/\varrho = \alpha dP/P - \delta dT/T$. According to (20.34) and (20.38), the variation of the central temperature, dT_c , is related to the variation of the central density, $d\varrho_c$, by

$$\frac{dT_c}{T_c} = \frac{4\alpha - 3}{3\delta} \frac{d\varrho_c}{\varrho_c}. \quad (28.1)$$

This defines a field of directions in the $\lg \varrho_c - \lg T_c$ plane as displayed in Fig. 28.1. Each arrow there indicates how T_c changes during contraction ($d\varrho_c > 0$). According to (28.1) the slope depends on the equation of state via α and δ . For an ideal gas $\alpha = \delta = 1$ and (28.1) becomes

$$\frac{dT_c}{T_c} = \frac{1}{3} \frac{d\varrho_c}{\varrho_c}. \quad (28.2)$$

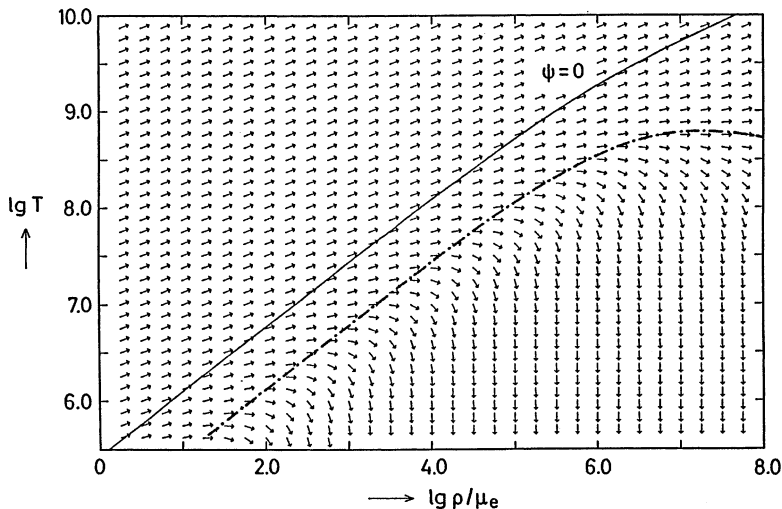


Fig. 28.1 The vector field given by (28.1) in a diagram showing the temperature T (in K) over the density ϱ/μ_e (in g cm^{-3}). The *arrows* indicate the direction in which the centre of a homologously contracting star would evolve. In the upper-left part the equation of state is that of an ideal gas, and therefore the arrows have a slope of $1/3$. The *thin solid line* at which the degeneracy parameter $\psi = 0$ indicates roughly the transition from the ideal gas to degeneracy of the electrons. The critical line along which $\alpha = 3/4$ is *dot-dashed*. On this curve the *arrows* point horizontally while below it the *arrows* point downwards

Here the slope is $1/3$, a contracting ideal gas heats up (the latter conforms with the conclusions drawn from the virial theorem in Sect. 3.1). The same slope also holds for non-negligible radiation pressure ($\beta < 1$) as can be seen if (13.7) is introduced into (28.1). In Fig. 28.1 the evolutionary track of a (homologously) contracting ideal gaseous sphere is a straight line with slope $1/3$. This necessarily leads closer to the regime of degeneracy, which is separated from that of ideal gas by a line of slope $2/3$ [see (16.6) and Fig. 16.1]. The onset of degeneracy changes α and δ and decreases the slope of the arrows in Fig. 28.1. In the limit of complete non-relativistic degeneracy one has $\alpha \rightarrow 3/5$ and $\delta \rightarrow 0$. What happens to a sphere which is contracting and becomes more and more degenerate? Then α will pass the value $3/4$ when δ is still finite and the slope given by (28.1) will change sign. Further contraction leads to cooling: the stronger the degeneracy the steeper will be the then negative slope, until finally the stellar centre tends to cool off at almost constant density. In the case of complete relativistic degeneracy, with $\alpha = 3/4$ and $\delta = 0$, the factor on the right of (28.1) becomes indeterminate. Then the ion gas - although its pressure is negligible compared to that of the degenerate electrons - will

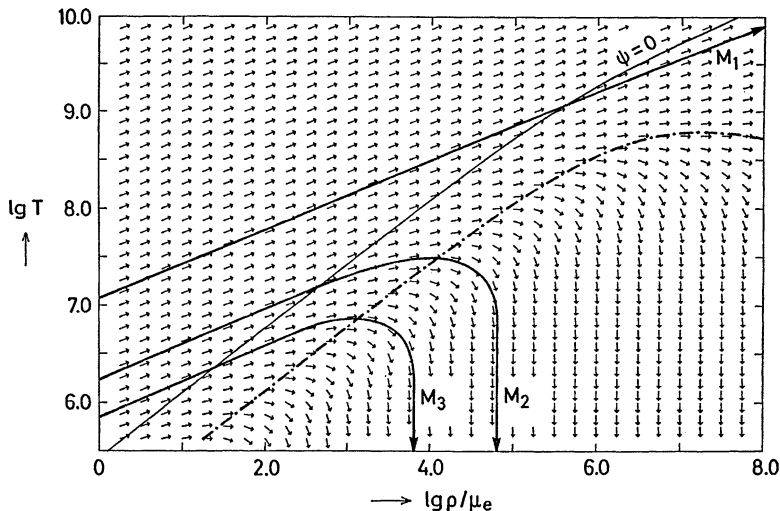


Fig. 28.2 Temperature T (in K) over density ϱ/μ_e (in g cm^{-3}) with the vector field and the lines $\psi = 0$ and $\alpha = 3/4$ as in Fig. 28.1. The heavy lines give the “evolutionary tracks” of the centres of three homogeneously contracting stars of different masses. Mass M_1 is so large that the evolution is not remarkably influenced by degeneracy, and the centre continuously heats up during contraction. For mass $M_2 (< M_1)$ degeneracy becomes important in the centre, and consequently a homologous contraction cannot bring the central temperature above a few 10^7 K (which is not sufficient to start helium burning). Mass $M_3 (< M_2)$ while contracting will start to cool off even before the temperature of hydrogen burning is reached

determine the slope. A dash-dotted line in Fig. 28.1 connects the points of vanishing slope ($\alpha = 3/4$).¹

For the sake of simplicity let us first ignore the fact that nuclear reactions set in at certain temperatures. Obviously, the evolutionary track of a contracting gaseous sphere in the $\lg \varrho_c - \lg T_c$ diagram depends very much on the starting point at the left-hand border, as can be seen from Fig. 28.2. If a stellar centre starts there sufficiently low it will reach a maximum temperature and begin to cool again after entering the domain of degeneracy. But if it started on the left at a sufficiently high temperature, it will never be caught by degeneracy and thus will continue to heat up.

Which types of spheres do reach a maximum temperature, and which types have the privilege of heating up forever? This depends on the mass of the sphere. In order to show this we consider two homologous spheres of an ideal gas with masses M and $M' = M/x$ and radii R and $R' = R/z$. Then, according to (20.9), $\varrho_c/\varrho'_c = xz^{-3}$, $P_c/P'_c = x^2z^{-4}$, and therefore, for an ideal gas, $T_c/T'_c = x/z$. If we now compare states in which the two spheres have the same central density ($xz^{-3} = 1$),

¹Since the dash-dotted line in Fig. 28.1 gives the impression of delineating a hill, this kind of figure is sometimes called *Thomas-mountain* after H.-C. Thomas who first used it to illustrate the evolution of homogeneously contracting stellar cores.

we have $T_c/T'_c = x^{2/3} = (M/M')^{2/3}$. This means that in Fig. 28.2 the evolutionary tracks of larger masses are above those of smaller masses. Consequently it is the less massive spheres which will finally be forced by degeneracy to cool off after having reached a maximum central temperature, being smaller the smaller the mass.

This has immediate consequences for the nuclear reactions, which we have ignored up to now. We know that a nuclear burning in a wide range of densities occurs at a characteristic temperature: hydrogen burning near 10^7 K and helium burning at 10^8 K (Since here we are discussing early phases of stellar evolution, we exclude the pycnonuclear reactions, which occur at extremely high densities only; see Sect. 18.4). One can therefore expect that a contracting sphere below a certain critical mass may never reach the temperature of hydrogen burning, since its central temperature never reaches 10^7 K. This is the case for M_3 in Fig. 28.2.

This important result deduced from simple homology considerations is also manifested in computer calculations of more realistic stellar models. Although the cores formed in the protostar phase do not contract completely homologously, their centres evolve in the $\lg \rho$ – $\lg T$ plane very similarly. Protostars of mass less than about $0.08M_\odot$ never ignite their hydrogen and thus never become main-sequence stars. These are the *brown dwarfs* we already introduced in Sect. 22.4. Here we have encountered an evolutionary aspect of the lower end of the main sequence: protostars born with too little mass never reach the state of complete equilibrium by which the main-sequence models are defined. Even if some nuclear reactions have started, they are so slow at these low temperatures that equilibrium abundances (rate of destruction = rate of production) of the involved nuclei are not reached even in the lifetime of the galaxy.

We shall see later that analogous considerations can be used to explain critical masses for the ignition of each higher nuclear burning in contracting cores of evolved stars. Helium burning is not reached by stars of an initial mass below approximately $0.5M_\odot$; for carbon burning, it has to be above $6M_\odot$. And masses above $\approx 8M_\odot$ will never be caught by degeneracy in this way (see Sect. 35.2).

28.2 Approach to the Zero-Age Main Sequence

We have seen that a contracting star of more than $0.08M_\odot$ ignites hydrogen in its centre and becomes a star on the zero-age main sequence (ZAMS). While the luminosity of the star was originally due to contraction, it now originates from nuclear energy. These two energy sources are quite differently distributed in the star. According to (20.41), $\varepsilon_g \sim T$ is not so much concentrated towards the centre, while hydrogen burning with $\varepsilon_{pp} \sim T^5$ and $\varepsilon_{\text{CNO}} \sim T^{18}$ has strong central concentration. Clearly the transition from contraction to hydrogen burning requires a rearrangement of the internal structure. The protostar becomes a zero-age main-sequence star with properties very close to those described in Chap. 22. The difference arises from the fact that some nuclear reactions, for example, the proton captures on ^2H , ^7Li , or ^{12}C , start at temperatures lower than those of core hydrogen burning.

The way in which nuclear reactions take over the energy production can now be followed by detailed numerical models following the approach to the main sequence of contracting protostars. We first discuss the results for one solar mass. Some reactions of the CNO cycle as given in (18.64) become important before the central temperature has reached that of equilibrium hydrogen burning (where the participating nuclei have equilibrium abundances). At a central temperature of about 10^6 K, all the ^{12}C that had been in the interstellar cloud will burn into ^{14}N via the reactions of the first three lines in (18.64). However, the following $^{14}\text{N}(p, \gamma)^{15}\text{O}$ reaction is much slower—and therefore often called the bottleneck reaction—such that the full CNO cycle cannot be completed. Once switched on, this process will take over the energy generation and stop the contraction. Because of the high temperature sensitivity of ε , the energy is released close to the centre. Consequently the energy flux $l/4\pi r^2$ is large, and a convective core that contains almost 10% of the total mass develops. At the same time, the first reactions of the pp chain become relevant, transforming H into ^3He [see the first two lines of (18.62)]. With decreasing ^{12}C the pp reactions become more important, and ^3He can be destroyed by $^3\text{He}+^3\text{He}$ and $^3\text{He}+^4\text{He}$ [the two reactions in the third line of (18.62)]. As a consequence the concentration of ^3He reaches a maximum at $m = 0.6M$. Outside, the temperature is too low to form ^3He , while inside, ^3He is used up to form ^4He . This characteristic shape of the ^3He abundance curve remains throughout the main-sequence evolution (see Fig. 29.3). With the depletion of ^{12}C in the central region the convective core disappears and the pp chain becomes the dominant energy source.

The situation is similar for more massive stars. But then instead of the pp chain, the CNO cycle finally takes over and the abundance of ^{12}C becomes that of equilibrium. For stars of $M > 1.5M_{\odot}$ the effect of pre-main-sequence ^{12}C burning can even be seen in the computed evolutionary tracks in the Hertzsprung–Russell diagram: there seems to be another, relatively short-lived main sequence to the right of the ordinary (hydrogen) main-sequence. Contracting protostars stay there until their ^{12}C fuel is used up before they move on to the main sequence. This somewhat prolongs the time a protostar needs to reach the ZAMS.

The numbers quoted here are from pre-main-sequence evolution calculations that ignore the detailed results of Chap. 27. They start out with a cool protostar on the Hayashi line and follow the ensuing quasi-hydrostatic contraction until the model reaches the hydrogen main sequence. The errors introduced by this simplification are not too large and certainly become negligible towards the end of pre-main-sequence contraction when the thermal history of accretion is forgotten by the star.

This has to do with the fact that, whatever the thermal history of the protostar, its structure has adjusted to thermal equilibrium after a Kelvin–Helmholtz time. Since the main-sequence timescale (which is relevant for the ensuing evolution) is much longer, the stars settle on the ZAMS quite independently of their past. Whatever their detailed history, tracks of protostars of the same mass and chemical composition lead to the same point on the ZAMS.

We now turn to the question of how rapidly stars of different M approach the ZAMS. Decisive for this is the Kelvin–Helmholtz timescale $\tau_{\text{KH}} \approx c_v \bar{T} M / L$. The mean temperature \bar{T} does not vary too much with M , since T_c is anyway just below

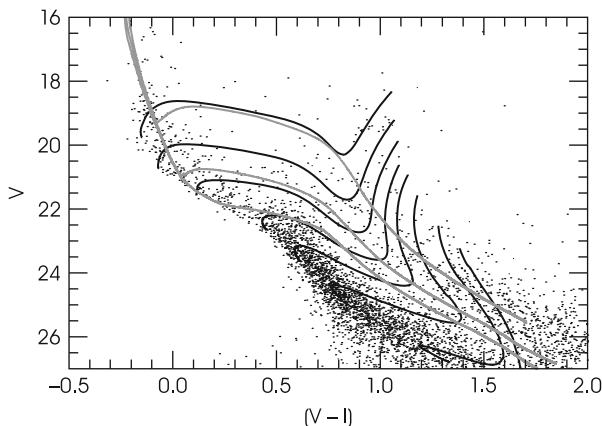


Fig. 28.3 Colour-magnitude diagram of the young open cluster NGC 602. The *dots* are the cluster stars. Overlaid are pre-main-sequence evolutionary tracks for masses between $3.0M_{\odot}$ and $0.5M_{\odot}$ (black lines; *top to bottom*) as well as isochrones obtained from these tracks with ages of 1, 5, and 10 Myr (grey lines; *top to bottom*) (After Cignoni et al. 2009)

the ignition temperature of hydrogen. As a rough estimate for L , we may take the corresponding ZAMS luminosity, since the evolutionary tracks in their final parts are at about that luminosity (see Fig. 27.5). Then $L \sim M^{3.5}$ and $\tau_{\text{KH}} \sim M^{-2.5}$. This means that massive protostars reach the ZAMS much faster than their low-mass colleagues.

In the Hertzsprung–Russell diagrams of very young stellar clusters one finds that only massive stars are on the main sequence, while the low-mass stars lie to the right of it. As an example we show in Fig. 28.3 the case of NGC 602 (Cignoni et al. 2009), a very young star cluster with a population of stars born only a few million years (Myrs). From comparison with low-mass pre-main-sequence evolutionary tracks and isochrones² it is obvious that many stars have not yet reached the main sequence. Similar cases in the Milky Way are the Pleiades (80 Myrs) and NGC 2264 (5 Myrs). It seems that, because of their longer τ_{KH} , these stars are still in the contraction phase and have not yet begun with nuclear burning. Among them are flare stars (UV Ceti stars), Herbig AE/BE, and T Tauri variables. The cause of their (irregular) variability is not yet fully understood, but is ascribed to circumstellar or chromospheric activity in connection with rotation as well as internal pulsations.

²An *isochrone* is the locus of stellar models of identical age, but different mass in the Hertzsprung–Russell diagram.